ISSN 1674-1056
http://cpb.iphy.ac.cn
http://iopscience.iop.org/cpb
中国物理 B
Chinese Physics
中国物理 Chinese Physics B

Magnetochemistry and chemical synthesis

Qianwang Chen(陈乾旺), Lin Hu, Guoliang Xia

Citation: Chin. Phys. B . 2019, 28(3): 037102. **doi:** 10.1088/1674-1056/28/3/037102
Journal homepage: http://cpb.iphy.ac.cn; http://iopscience.iop.org/cpb

What follows is a list of articles you may be interested in

Heavy fermions in high magnetic fields

M Smidman, B Shen(沈斌), C Y Guo(郭春煜), L Jiao(焦琳), X Lu(路欣), H Q Yuan(袁辉球)

Chin. Phys. B . 2019, 28(1): 017106. **doi:** 10.1088/1674-1056/28/1/017106

Pressure effect in the Kondo semimetal $CeRu_4Sn_6$ with nontrivial topology

Jiahao Zhang(张佳浩), Shuai Zhang(张帅), Ziheng Chen(陈子珩), Meng Lv(吕孟), Hengcan Zhao(赵恒灿), Yi-feng Yang(杨义峰), Genfu Chen(陈根富), Peijie Sun(孙培杰)

Chin. Phys. B . 2018, 27(9): 097103. **doi:** 10.1088/1674-1056/27/9/097103

Voltage-controlled Kosterlitz-Thouless transitions and various kinds of Kondo behaviors in a triple dot device

Yong-Chen Xiong(熊永臣), Jun Zhang(张俊), Wang-Huai Zhou(周望怀), Amel Laref

Chin. Phys. B . 2017, 26(9): 097102. **doi:** 10.1088/1674-1056/26/9/097102

Anisotropic and mutable magnetization in Kondo lattice $CeSb_2$

Yun Zhang(张云), Xiegang Zhu(朱燮刚), Bingfeng Hu(胡丙锋), Shiyong Tan(谭世勇), Donghua Xie(谢东华), Wei Feng(冯卫), Qin Liu(刘琴), Wen Zhang(张文), Yu Liu(刘瑜), Haifeng Song(宋海峰), Lizhu Luo(罗丽珠), Zhengjun Zhang(张政军), Xinchun Lai(赖新春)

Chin. Phys. B . 2017, 26(6): 067102. **doi:** 10.1088/1674-1056/26/6/067102

Electronic structure and magnetic properties of rare-earth perovskite gallates from first principles

A Dahani, H Alamri, B Merabet, A Zaoui, S Kacimi, A Boukortt, M Bejar

Chin. Phys. B . 2017, 26(1): 017101. **doi:** 10.1088/1674-1056/26/1/017101

TOPICAL REVIEW — Fundamental research under high magnetic fields

Magnetochemistry and chemical synthesis

Lin Hu(胡林)[1,†], Guoliang Xia(夏国良)[2], and Qianwang Chen(陈乾旺)[1,2]

[1] *Anhui Province Key Laboratory of Condensed Matter Physics at Extreme Conditions, High Magnetic Field Laboratory, Chinese Academy of Sciences, Hefei* 230031, *China*

[2] *Hefei National Laboratory for Physical Science at Microscale, Department of Materials Science & Engineering, University of Science and Technology of China, Hefei* 230026, *China*

(Received 8 January 2019; revised manuscript received 15 January 2019; published online 26 February 2019)

High magnetic field is one of the effective tools to control a chemical reaction and materials synthesis. In this review, we summarized the magnetic field effects on chemical reactions, such as reaction pathway, growth behavior of nanomaterials, product phase, and magnetic domain of materials. The surface spins and activity of catalysts under magnetic fields were also discussed.

Keywords: magnetochemistry, magnetic field effects

PACS: 71.27.+a, 74.25.Ha **DOI:** 10.1088/1674-1056/28/3/037102

1. Introduction

Traditionally, the magnetic field has been considered as a significant means to investigate the magnetic properties of materials for a long time. With the rapid progress of science and technology, magnetic fields gradually penetrate from the pure physics to chemistry, biology, medicine, and many other fields. The combination of magnetic fields and chemical reactions, to study the effect of magnetic field on reactions, is one of the important achievements, which leads to the creation of a new discipline, named as spin chemistry. The electronic spin and nuclear polarization during the chemical reaction process were mainly focused on by the spin chemistry, which could be described by the radical pair mechanism. Nowadays, a wide variety of magnetic field effects (MFEs) on chemical reactions are investigated in various chemical systems with the magnetic field intensities from 10 T down to lower than 1 T. As a result, the reaction rate, yield, structure, and distribution of the final product can be effectively controlled by the MFEs.

Since the late 1960s, the MFEs played on the chemical reaction kinetics have been extensively investigated.[1] Under the magnetic field of 1 T, the yield of lactam was minimum when the isoquinoline *N*-oxide was irradiated in ethanol.[2] At room temperature, the hydrogen abstraction reaction was also investigated under magnetic fields. It was found that the benzophenone ketyl radical exhibited a lower escape yield when the intensity increased from 0 T to 10 T.[3] In 1989, an adequate and clearly structured description on MFEs in magnetokinetics was shown by Thomas Ulrich *et al.*[1] The important roles of magnetic fields played in radical reactions were reviewed by Brian Brocklehurst in 2002.[4] In 2009, the MFEs in chemical systems were summarized by Christopher T. Rodgers.[5] It is worth mentioning that the magnetochemistry has long been an activate research field.

Although the study of magnetochemistry in China started late, in recent years, the research appears as a tree with several branches.[6] Wan *et al.* reported the electrochemical polymerization of polyaniline under the applied magnetic field in 1995.[7] Ma *et al.* also demonstrated the MFEs on the free radical polymerization process of aniline, which showed that the polymerization rate, molecular weights, conductivity, and solubility enhanced under magnetic fields. Hu *et al.* showed the abnormal MFEs and possible mechanism for magnetizing charge-transfer complexes within reaction zone in an electrochemical system.[8,9] Fu *et al.* demonstrated that the MFEs could promote the efficiency of photocatalytic degradation of benzene during the process of photocatalysis. Overall, the magnetochemistry in China is just emerging, and there is still much room for development, especially associate with high magnetic fields. On the other hand, the current research mainly focuses on the experimental phenomena, leading to the lack of theoretical innovations. Moreover, in recent years, the research in magnetochemistry is expanding to material synthesis due to the development of materials science. The influence of magnetic fields on the physical and chemical processes of material formation has drawn much attention, which involves the regulation of materials structure at each level, such as morphology, phase, crystal structure, and so on. Nowadays, the synthesis method referring to magnetic fields has been a significant research topic in magnetochemistry. Here, a series of typical developments MFEs on chemical systems will be illustrated, which involves the reaction pathway, product phase, magnetic domain, growth behavior, and so on (Fig. 1).

[†]Corresponding author. E-mail: hulin@hmfl.ac.cn

© 2019 Chinese Physical Society and IOP Publishing Ltd

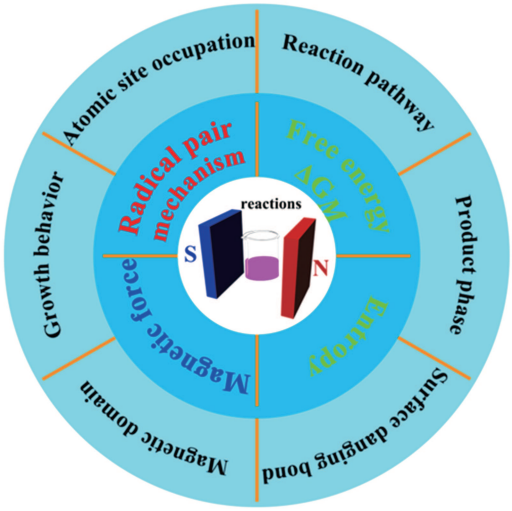


Fig. 1. Schematic illustration of MFEs on the chemical synthesis, inner core: chemical reactions under a magnetic field, shell: the ways in which a magnetic field may affect a reaction, outer shell: results caused by a magnetic field.

2. Theoretical background

As we know, the transport of matter and energy is involved during the chemical synthesis processes. Under magnetic fields, the changes in ions movement and related energy are produced. It is necessary to introduce theoretical backgrounds for better understanding the phenomena observed in this field.

2.1. The radical pair mechanism

The generation of spin-correlated radical pairs is the typical characteristic in the radical pair mechanism. Usually, the radical pair produced by an electronically excited triplet state will not recombine due to the energetic reason. As a result, the diamagnetic ground-state product with a singlet spin multiplicity can be produced, leading to the spin-forbidden condition for the recombination of initial radical pairs. However, after the separation of two radicals, the spin evolution originated from the dynamic state of the radical pair may eventually cause a singlet correlated state of electron spins, which leads to the recombination of the radical pair at the next reunion. The chemical reaction involved cage recombination or geminate recombination will compete with the final radical separations. The spin evolution rate is an important factor in determining the ratio of cage to the escape reaction yields, which depends on an applied magnetic field. Therefore, the reaction kinetics is related to the magnetic field. Overall, the spin evolution between singlet and triplet states, in which the rate and extent are affected by the magnetic field, is the key feature for radical pair mechanism. The MFEs lead to the yield changes of singlet product (SP) and triplet product (TP). A weak magnetic field can also lead to remarkable yield changes of SPs even interaction energies of weak magnetic fields are much lower than the thermal energy $k_{\mathrm{B}}T$. This result does not violate the laws of thermodynamics because much more than the thermal energy $k_{\mathrm{B}}T$ are required for the generation of radical pairs. Even though the magnetic interactions with weak fields in singlet and triplet states interconversion are tiny, the product yield may be also remarkably changed. Undoubtedly, the magnetic interactions under high magnetic fields will bring more remarkable changes. Many original and review papers explained the principles of the radical pair mechanism in detail.[1,4,5]

2.2. Magnetic energy

Based on thermodynamics, the early theoretical arguments suggested that the chemical transformation should be promoted by magnetic fields in a chemical reaction. However, there are no significant impacts to be seen on these grounds according to a quantitative estimation of Gibbs free enthalpy produced by a magnetic field. The ΔG_{M}, defined as the free enthalpy of a reaction produced by a magnetic field at field strength of B_0 in vacuum, could be expressed as follows:

$$\Delta G_{\mathrm{M}} = -(1/2)\Delta\chi_{\mathrm{M}}B_0^2,$$

where $\Delta\chi_{\mathrm{M}}$ is the magnetic susceptibility change of one molar unit during the reaction.[1] For example, based on a value of 0.01 $\mathrm{cm^3/mol}$ (corresponds to consumption or production of 5 $\mu_{\mathrm{B}}\cdot\mathrm{mol}^{-1}$), $\Delta G_{\mathrm{M}} = 0.05\ \mathrm{J\cdot mol^{-1}}$ could be obtained under a field of 1 T, which means a factor of 10^{-5} for the equilibrium constant change at room temperature. However, when the chemical reactions occur in high magnetic fields, such as pulsed magnetic field up to 100 T, the ΔG_{M} is considerable. In this case, ΔG_{M} may be a significant factor to determine the direction of room temperature chemical reactions. Moreover, the rate of chemical reaction is not only determined by the energy, but also by the entropy. According to quantum mechanics, chemical reaction depends on electron spin. The spin of unpaired electrons involved in the chemical reaction can be influenced by a magnetic field, thus changing the entropy of the reaction system.

2.3. Magnetic force

Under magnetic fields, when the species with a charge move at a velocity in chemical reaction systems, a force will be produced. The force $\boldsymbol{F}_{\mathrm{L}}$, named as the Lorentz force, can be expressed by Lorentz equation $\boldsymbol{F}_{\mathrm{L}} = q\boldsymbol{v}\times\boldsymbol{B}$. As we know, the Lorentz force acts on one in the direction that is related with the charge sign and perpendicular to the direction of $\boldsymbol{v}$ and $\boldsymbol{B}$.

3. Chemical reaction under magnetic field

3.1. MFEs on reaction pathway

The self-assembly chemical synthetic method is the main strategy for constructing the molecule-based magnets by a se-

lection of proper spin source and associated structures. Usually, transition metal ions or organic radicals provide the spin source, while the associated structures are composed of coordinating ligands. The self-assembly process is dependent on the inner driving force, which is hard to adjust. As a kind of exterior driving force, the magnetic field is expected to influence the chemical reaction involved transition metal ions and organic radicals.

Our group has shown the MFEs on the pathway in a ligands reaction system.[10] The hydrothermal synthesis reactions which involve the coordinating ligands of isonicotinic acid and sodium azide were carried out. When no magnetic field was applied, the final product contained ca. 5% red crystals with the chemical formula of $[Co_{1.5}(N_3)(OH)(L)]_n$ (Fig. 2(b), antiferromagnetism) and 95% yellow crystals (Fig. 2(a), paramagnetism). However, the yield of red crystals raised to 25% under the magnetic field of 0.2 T. Obviously, the applied magnetic field favors to form the crystals with antiferromagnetism. The activation energy of the antiferromagnetic complex is expected to decrease during the chemical reaction process because of the magnetic field. Based on the final product, it is deduced that two transition states (chemical reaction pathways) which could be expressed as $[Co\ldots L\ldots H_2O]$ and $[Co\ldots L\ldots OH^-\ldots N_3^-]$ were involved during the reaction process. Without a magnetic field, the main product is yellow crystal, which indicates that the activation energy of $[Co\ldots L\ldots H_2O]$ is lower than that of $[Co\ldots L\ldots OH^-\ldots N_3^-]$. However, the activation energy of $[Co\ldots L\ldots OH^-\ldots N_3^-]$ can be reduced largely when a magnetic field is applied. The red crystals hold short-range antiferromagnetic coupling interaction and mainly show antiferromagnetism according to the magnetic measurement result. Under a magnetic field, the magnetic exchange can be efficiently mediated in $[Co\ldots L\ldots OH^-\ldots N_3^-]$ activated complex which possesses bridging ligands, leading to producing a direction of magnetic phase transition between paramagnetic and antiferromagnetic states. This magnetic phase transition is attributed to the lower energy of antiferromagnetic phase compared to that of paramagnetic phase. Moreover, for the same material, compared to the paramagnetic phase, the antiferromagnetic phase is more stable under a magnetic field. Due to this transition, based on the viewpoint of thermodynamics, the self-assembly reaction will process more easily because of the decreased activated energy of the activation complex. However, under a magnetic field, no phase transition takes place for the yellow crystal with the paramagnetic property. Therefore, the activation energy of the yellow crystal is maintained (Fig. 3). Moreover, during a Ni-complex reaction process, a magnetic field of 0.3 T can totally change the final product from green into blue (Fig. 2(c)),[11] which means that the reaction pathways can be selected by a magnetic field.

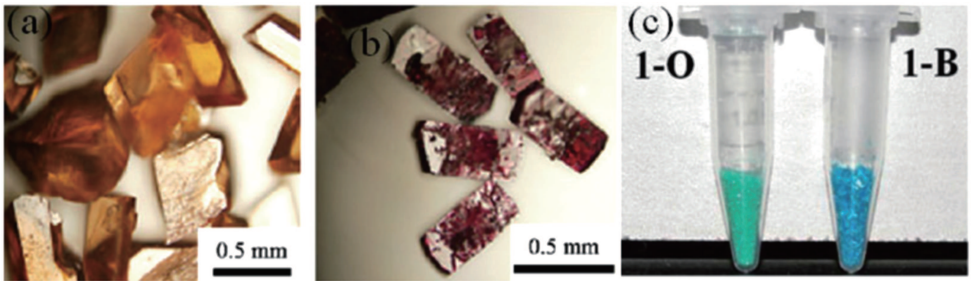


Fig. 2. Optical images of the products: (a) yellow crystals, (b) red crystals, and (c) 1-O: green, 1-B: bule.[10,11]

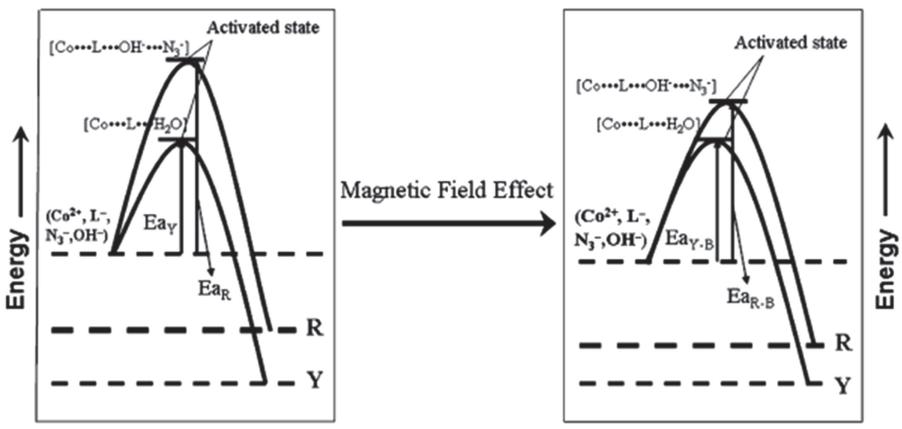


Fig. 3. Scheme of the MFEs on activation energies of the self-assembly reaction.[10]

As we know, organic ligands possess various coordination modes. In other words, there are several reaction pathways during the self-assembly process. The above results show that magnetic fields may be a strategy to control the reaction pathways of molecule-based magnets. A magnetic field with higher intensity is expected to bring more significant changes, and even exploring the new molecule-based magnets with high performance.

3.2. MFEs on product phase

In general, it is considered that MFEs on product phase will occur in organic chemical reactions. However, many research confirmed that the product phase of some inorganic chemical reactions can be influenced by the magnetic field. Ma *et al.* showed that the product phase of Fe_2O_3 could be changed under a magnetic field of 12 T during the chemical reaction process at 500 °C.[12] Without a magnetic field, the XRD pattern of the product is consistent with that of single phase α-Fe_2O_3. However, the major peaks of XRD patterns of the magnetic field-induced products can be indexed to γ-Fe_2O_3 with a cubic spinel phase, indicating that γ-Fe_2O_3 has been fabricated under 12 T (Fig. 4). It is suggested that the magnetic field, like temperature, can change the free energy during chemical reaction processes based on the thermodynamic viewpoint. Therefore, in the presence of a magnetic field, there are two aspects free-energy in the reaction system. In addition to the thermal Gibbs free energy $\Delta G_{\mathrm{T}}(T)$, the magnetic field also produces the free energy which can be defined as the magnetic Gibbs free energy $\Delta G_{\mathrm{M}}(T,H)$. The combination of ΔG_{T} and ΔG_{M} is the total Gibbs free energy for the phase transformation from α-Fe_2O_3 to γ-Fe_2O_3. The ΔG_{M} can be attributed to the difference magnetic susceptibilities of γ-Fe_2O_3 and α-Fe_2O_3. The ΔG_{M} can be estimated with the following formula:

$$\Delta G_{\mathrm{M}} = -\frac{1}{2}\mu_0\left(\chi_\gamma - \chi_\alpha\right)H^2,$$

where χ_α and χ_γ are the magnetic susceptibilities of α-Fe_2O_3 and γ-Fe_2O_3 at a temperature, respectively. The μ_0 represents the permeability of free space, and H is the applied magnetic field intensity. At 500 °C, ΔG_{M} is negative because χ_γ is larger than χ_α, leading to the decrease of the total free energy $(\Delta G_{\mathrm{T}} + \Delta G_{\mathrm{M}})$ under the applied magnetic field. As a result, a great tendency which favors to form γ-Fe_2O_3 phase has been produced under the field intensity of 12 T. According to the above analysis, the fabrication of γ-Fe_2O_3 is mainly attributed to magnetic energy based on thermodynamic perspective. Obviously, the ΔG_{M} produced from magnetic fields can be a factor to determine the product phase. Recently, a high magnetic field was also applied to induce the formation of Mn_3O_4 via a hydrothermal reaction. The stability of the chemical reaction could be destroyed by a static magnetic field, which has been proved by the experiment results and magnetic measurements. As a result, the reaction pathway was changed to form the higher magnetism product. Moreover, the Gibbs energy produced by the magnetic field is responsible for the formation of Mn_3O_4 based on the thermodynamic calculation.[13]

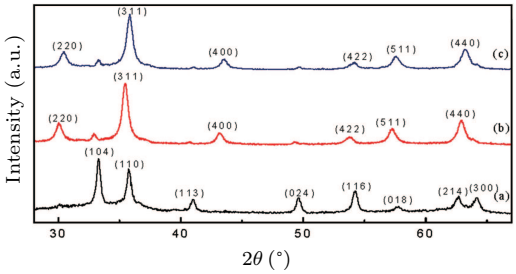


Fig. 4. The XRD patterns for the products obtained at the temperature of 500 °C under no magnetic field (a) and 12 T: (b) $B\perp$ the sample and (c) $B \parallel$ the sample.[12]

Moreover, Yu *et al.* demonstrated the fabrication of ferrosulfide minerals assisted by the magnetic field, which showed that the MFEs could effectively change the phase of the product.[14] At 180 °C, without a magnetic field, a product composed of Fe_3S_4, and FeS_2 was obtained, while a metastable phase of pure cubic Fe_3S_4 could be formed under a magnetic field of 0.045 T. The free energy produced by the magnetic field is the main factor to determine the formation of cubic Fe_3S_4 (ferromagnetic phase). Interestingly, pure cubic Fe_3S_4 was also formed under no magnetic field at a relative low temperature of 160 °C, which further proves the similar effect of the magnetic field and temperature.

The semiconducting phase (2H) of MoS_2 is constructed by two S–Mo–S layers while the metallic phase (1T) is built by a single S–Mo–S layer. The 1T phase has emerged as an attractive candidate for wide applications and is expected to exhibit better performance than its semiconducting counterpart due to its high electrical conductivity, exotic ferromagnetic behavior, and superconductivity. Therefore, obtaining the MoS_2 nanostructure with a high concentration of 1T phase is a significant strategy to realize the enhanced properties. A new strategy, named as high magnetic field-induced method for synthesizing stable 1T phase MoS_2 nanosheets, has been demonstrated. When the magnetic field intensity reaches 9 T in the reaction system, the stable metallic phase concentration as high as $\sim 100\%$ can be successfully achieved in MoS_2 nanosheets. Interestingly, the 1T phase concentration is related with the magnetic field intensity. The 1T phase percentage of the MoS_2 nanosheets synthesized under 0 T, 5 T, 8 T, and 9 T is estimated to be $\sim 25\%$, 50%, 75%, and 100%, respectively. As we know, the Mo^{4+} in 2H phase shows the trigonal prismatic local coordination, which leads to the zero net magnetic moment because of two spin-antiparallel 4d electrons. As a result, the 2H phase of MoS_2 is macroscopically nonmagnetic. In contrast, the magnetic moment of 1T-MoS_2

is 2 μ_B/Mo ion. Therefore, 1T phase incorporation in 2H phase will display ferromagnetism at room temperature. At 300 K, the measured saturation magnetizations (M_s) of the as-prepared MoS_2 nanosheets obtained under 0 T, 5 T, 8 T, and 9 T are 0.005 emu/g, 0.013 emu/g, 0.017 emu/g, and 0.022 emu/g, respectively. It should be noted that the value of M_s agrees with the ratio of 1T phase and 2H phase. These results indicate that the applied magnetic fields can promote the fabrication of magnetic materials during the reaction process.

Based on the experimental results, the possible mechanism is deduced as follows. Without applied magnetic fields, the as-prepared MoS_2 nanosheets contain $\sim 25\%$ 1T phase, which are similar to the MoS_2 nanosheets obtained by the two-step hydrothermal synthesis.[15] The 1T phase tends to appear near the edge of the 2H phase MoS_2 nanosheets as previous reports.[16] Under a high magnetic field, a strain can be produced because of the nonzero magnetic moment of 1T phase. As a result, the original MoS_2 lattice inevitably undergoes a structural distortion due to the strain, which will lead to the MoS_2 nanosheets become thinned, resulting in the transformation of the 2H phase into 1T phase. The driving force of this process mainly arises from the magnetic fields, which may be defined as magnetic exfoliation. With the increase of the magnetic field intensities, the strength of the strain will be increased, resulting in the enhanced concentration of 1T phase in MoS_2 nanosheets. Also, another explanation is considered. The previous report showed that pure 1T MoS_2 was obtained by a hydrothermal synthesis process at 200 °C while 2H MoS_2 was formed at 240 °C.[17] This is because the octahedral structure of 1T MoS_2 cannot be maintained under the growth conditions used, such as temperature at 240 °C. Similarly, without high magnetic fields, the 1T MoS_2 formed during synthesis process may easily transform to 2H MoS_2. However, the octahedral coordination of 1T MoS_2 may be maintained under the assistant of high magnetic fields, resulting in the high concentration of 1T MoS_2 in the product.

3.3. MFEs on electrochemical reaction

In electrochemical reactions, the MFEs on electrogenerated chemiluminescence (MFE_{ECL}) intensity, which can be generated through density and conversion channels, have been widely employed to study spin-dependent reaction routes (Fig. 5(a)). In the density channel, it is shown that the density of light-emitting states can be changed under a magnetic field due to the existence of magnetizing and Lorentz forces on the reactant radicals. Under a magnetic field, in the conversion channel, the spin mixing may modify the conversion between singlets and triplets in both light emitting states and intermediate charge-transfer complexes. In the electrochemical reaction, a considerable MFE_{CEL} intensity with the amplitude less than 30% has been achieved in early experimental studies. Using a conveniently controllable electrochemical co-reaction, Hu *et al.* reported a giant MFE-CEL with a magnitude larger than 400% based on Lorentz force effects in liquid states[9] (Fig. 5(c)). During the electrochemical oxidation catalytic process, the tripropylamine (TPrA) acts as an co-reactant for $Ru(bpy)_3^{2+}$. In the $Ru(bpy)_3$-based electrochemical reaction, a giant MFE_{CEL} can be generated at different electrical biases under a two-electrode electrochemical configuration in which an external magnetic field is applied. Under the field intensity of 0.07 T, the MFE_{CEL} can reach 400% at 3.3 V. This result is much larger than the MFE_{CEL} reported previously. The observed giant MFE_{CEL} is mainly attributed to the existence of the Lorentz

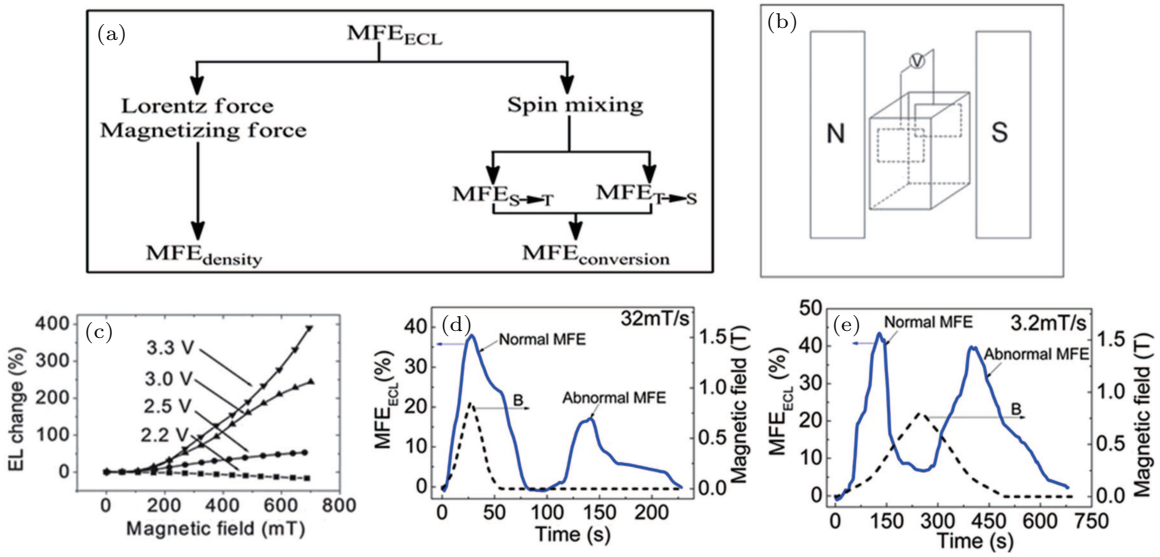


Fig. 5. (a) MFE_{ECL} is generated by density and conversion channels. (b) Experimental setup with a two-electrode configuration or an electrochemical cell placed in a magnetic field. (c) MFE_{CEL} at different voltages. (d) Normal and abnormal MFE_{ECL} under fast field-sweeping rate of 32 mT/s. (e) Normal and abnormal MFE_{ECL} under fast field-sweeping rate of 3.2 mT/s.[8]

force effects which can cause the convection for the reactive species in the liquid solution by the momentum transfer between the solvent molecule and reactive ion. The convection generated by the Lorentz force will promote the ion penetration through diffusion layer in the electrochemical reaction. Moreover, the decrease of the diffusion layer thickness is achieved. The electrochemical reaction can be enhanced due to the increase of ion penetration, which increases the electroluminescence intensity. As a result, a positive MFE_{CEL} is observed. Moreover, in liquid states, it is suggested that regulating the Lorentz force effects to a proper level will present a novel strategy to gain giant MFEs based on the electrochemical reaction.

In early researches, it was found that the normal MFE_{ECL} appeared in the electrochemical system with the existence of magnetic fields (Fig. 5(b)). Based on the electrochemical system of $Ru(bpy)_3Cl_2$-TPrA, for the first time, Hu *et al.* observed the abnormal MFE_{ECL} after removing the applied magnetic field,[8] which may be attributed to the magnetized state of the charge-transfer $[Ru(bpy)_3^{3+}\ldots TPrA^{\bullet}]$ complex and experience the magnetic relaxation with long time. The magnetized state of the charge-transfer complex is confirmed by the distinct behavior between magnetocurrent and MFE_{ECL}, which is responsible for the abnormal MFE_{ECL} from an electrochemical system. The magnetic coupling between the charge-transfer complexes with the magnetic relaxation may be revealed by the experimental results on abnormal MFEs in solution.

3.4. MFEs on growth behavior of nanomaterials

Because the properties of materials or performances of devices mainly depend on structures, it is significant to control the size, shape, and microstructure of nanomaterials in modern science and engineering. The recent research shows that the growth behavior of both the ferro/ferromagnetic and paramagnetic/diamagnetic nanomaterials can be tailored by magnetic fields during the chemical synthesis process, which leads to great change of the as-prepared product.

For magnetic materials, the oriented growth can be induced by a magnetic field. As a result, the material will grow along the easy magnetic axis to form one-dimensional nanostructure. In 2004, for the first time, Chen *et al.* showed the growth of Fe_3O_4 nanowires with single crystalline feature under a magnetic field, which was carried out in a self-made autoclave with cylindrical NdFeB magnets.[18] Without an applied magnetic field, Fe_3O_4 particles with hexagonal and square shapes were observed. Interestingly, under a field intensity of 0.35 T, a fibrous nanostructure and nanowires were obtained at a large scale. Meanwhile, the aquare particles disappeared (Figs. 6(a) and 6(b)). The electron diffraction (ED) pattern combined with the HRTEM results indicated that the Fe_3O_4 nanowire was single crystalline and grew along the easy magnetic axes of [110] (Figs. 6(c) and 6(d)). It is suggested that the Lorentz force produced by the magnetic field can influence the behavior of individual ions, leading to the preferential nucleation of particles during the growth process. Moreover, under magnetic fields, metallic nickel wires with width diameter fluctuation were obtained by chemical reduction of $[Ni(N_2H_4)_x]^{2+}$ complexes. The magnetic attraction generated from the magnetic field can lead to the alignment of $[Ni(N_2H_4)_x]^{2+}$ complexes along the lines of magnetic force. As a result, the chemical reduction of $[Ni(N_2H_4)_x]^{2+}$ complexes will occur along the lines of magnetic force to form metallic nickel wires. It is worth mentioning that the magnetic field-induced method could be recommended as one of the six ways to form nanowires.

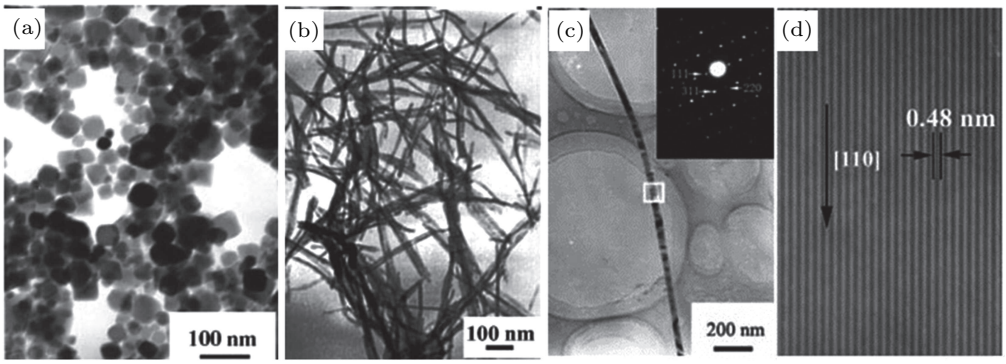


Fig. 6. TEM images of the samples obtained in zero magnetic field (a) and 0.35 T (b), (c) TEM image of a typical Fe_3O_4 nanowire, (d) HRTEM image of the nanowire obtained under a magnetic field.[18]

The magnetic field with a low intensity may generate negligible effects on the growth of paramagnetic or diamagnetic structures during the chemical synthesis process. However, the MFEs are related with the magnetic field intensity according to the formulas. Therefore, for the nanostructures of weak magnetic materials, a high magnetic field needs to be applied in the chemical reaction systems for tailoring the growth behavior. Carbon filaments were prepared by the scientists in Japan and

Israel under the field intensity of 10 T.[19] The paramagnetism and large diamagnetic anisotropy of graphitic clusters were caused by the localized spins which appeared in large numbers at the boundaries of graphitic plane edges, which must be related to the growth induced by a magnetic field. Moreover, a magnetic field-assisted approach to fabricate Bi nanowires has been demonstrated.[20] The Bi microspheres with different diameters were obtained under the zero magnetic field (Fig. 7(a)). Evidently, the morphology remarkably changed when the magnetic fields were applied during the synthesis process. A small amount of nanowires were formed under the magnetic field of 1 T (Fig. 7(b)). When the strength reached 4 T, many nanowires combined with nanobelts were fabricated (Fig. 7(c)). Under the magnetic field of 8 T, a large number of Bi nanowires could be observed (Fig. 7(d)), accompanied by the disappearance of other morphologies. The representative HRTEM image showed that the as-prepared nanowire is single crystalline (Fig. 7(e)). To some extent, the MFEs could change the surface energy of Bi nucleus when the synthesis process was progressed under a magnetic field with high intensity. However, the different axes of Bi possess distinct magnetic susceptibilities. As a result, along each axis, the MFEs induced surface energy changes are different. Based on the magnetic susceptibilities of each axis, it is deduced that the *c*-axis possesses the higher increase of surface energy compared to other axes. Moreover, because the energy of the (0001) plane is highest, the growth perpendicular to this high energy plane can be induced to decrease the system energy (Fig. 7(f)).

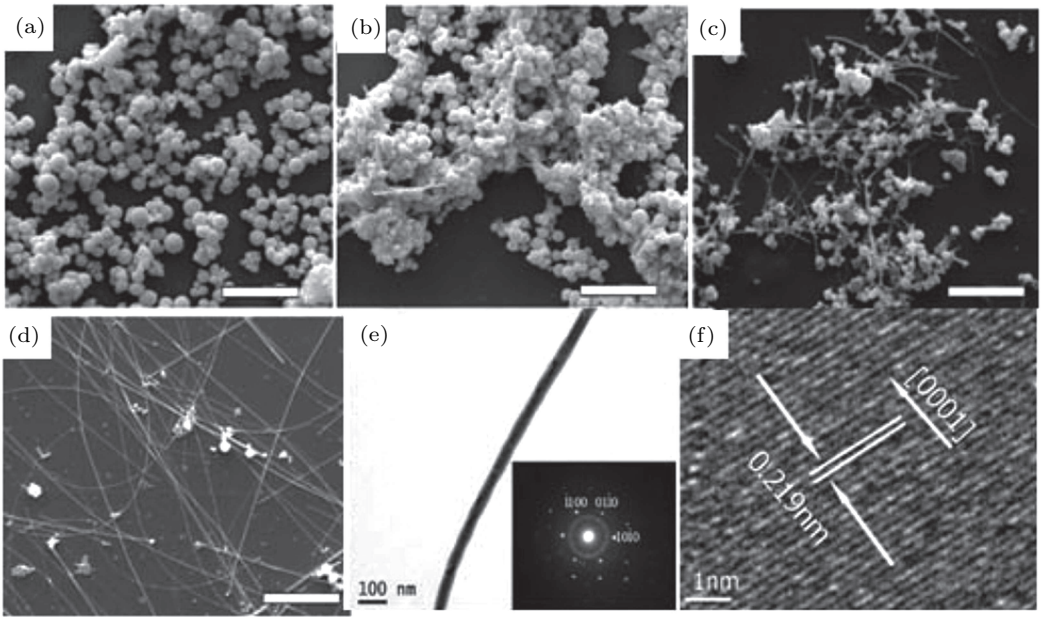


Fig. 7. The representative SEM images of Bi nanomaterials formed under diverse field strengths with scale bar of 5 μm: (a) 0 T, (b) 1 T, (c) 4 T, (d) 8 T. (e) The representative TEM image of the nanowire formed under 8 T, the inset is the SAED pattern of the nanowire. (f) The HRTEM image of a nanowire formed under 8 T.[20]

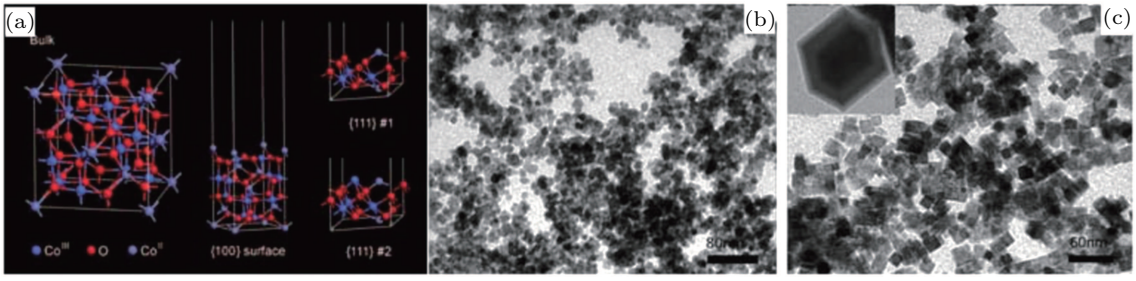


Fig. 8. (a) Structures of bulk Co_3O_4 and surface models for Co_3O_4 {100} and {111}. (b) and (c) The TEM images of Co_3O_4 particles obtained in the absence and presence of a magnetic field.[21]

Moreover, the experimental and theoretical researches have been carried out to investigate the MFEs on the surface energy during the process of nanoparticle growth.[21] Experimental results showed that the morphology of Co_3O_4 nanoparticles could be changed from irregular spheres into nanocubes when the chemical synthesis occurs under a magnetic field (Fig. 8). As we know, for the spinel structure, the morphology of Co_3O_4 nanoparticles is depended on the surface energies which are related with the competitive growth between different faces. The energies of {111} and {100} faces with and without applied magnetic fields were calculated. Without the field, the energy of the {100} faces (1.849 $J \cdot m^{-2}$) is higher

than that of the {111}#1 faces (1.645 J·m^{-2}) and {111}#2 (1.638 J·m^{-2}). However, under a magnetic field of 0.4 T, the energy of the {100} faces (1.326 J·m^{-2}) becomes lower than that of the {111}#1 faces (1.429 J·m^{-2}) and {111}#2 (1.447 J·m^{-2}). Obviously, under the applied magnetic field, the energies of both faces decrease, however, the reduction extent of {100} faces is larger than that of {111} faces. As a result, due to the relatively lower face energy, the {100} faces turn to be a growth limited form, leading to the change of the final morphology.

3.5. MFEs on magnetic domain structure

A lot of attention has been paid to the magnetic domain structure of one-dimensional materials due to the promising properties and applications as high density magnetic recording media. The magnetic force microscopy (MFM) has been employed to investigate the domain of one-dimensional nickel nanostructure with different diameters obtained under 0.25 T.[22,23] A single domain state was observed on the wire with the diameter of 250 nm, which is proved by the uniform dark contrast shown in Figs. 9(a) and 9(b). Moreover, the domain structure strongly associated with the diameter of the wires. In the wire with the diameter of 2 μm, the cylindrical domain with a unique core–shell structure was clearly observed, which is proved by the dark middle part and bright shell, as shown in Figs. 9(c) and 9(d). These results suggested that the unique multidomain can be aroused under an applied field during the reaction process. As mentioned above, under the magnetic field, nickel crystallites will grow along the lines of magnetic force to form the nickel wires in which the magnetic moments are lined in the same direction, leading to the formation of a single domain in the thin wire. In contrast, the exchange energy is increased in multi-domain configurations due to the unparallel spins of the inside domain walls. Moreover, the magnetization of the inside domain wall shifts away from the easy axis, leading to the increase of the magnetic anisotropy energy. In the wires with large diameters, the increase of anisotropy and exchange energy will be smaller than the decrease of magnetostatic energy, which results in the formation of multi-domains. For nickel wires with large diameters, a cylindrical core–shell multidomain in which the magnetic moments in the core possess the same magnetization and in the shell have the opposite magnetization will be formed to minimize the energy of the nickel wires. As shown in Fig. 9(e), the core possesses the magnetic moments with a downward direction, while an upward direction is observed for the moments of the shell.

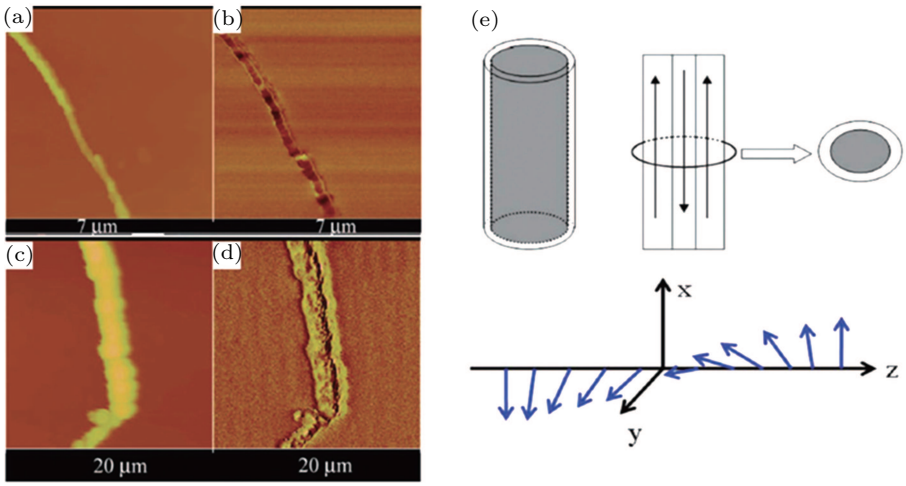


Fig. 9. The AFM and MFM images of the as-prepared nickel wires with different diameters under 0.25 T: (a), (b) 250 nm, (c), (d) 2 μm, (e) the graphical representation of the core–shell cylindrical domain layout.[22]

3.6. MFEs on structure at atomic scale

The Verwey transition (T_V), which is defined as the sharp and first order transition in magnetite on cooling below 120 K due to the charge ordering of the Fe^{3+} and Fe^{2+} in alternating layers on octahedral sites, was discovered in 1939. As we know, Fe_3O_4 nanoparticles experience a Verwey transition at approximately 120 K. Interestingly, this Verwey transition vanishes in Fe_3O_4 nanoparticles obtained under a field intensity of 0.25 T.[24] Figure 10 is the EPR spectra at low temperatures of the samples obtained with and without magnetic fields. The transition is clearly showed for the sample obtained without a magnetic field, which is proved by the reduced signal with the lowering of temperature and a sudden decrease near 120 K, as shown in Fig. 10(a). In contrast, the Verwey transition vanishes in the product obtained by a similar way under 0.25 T (Fig. 10(b)). The Mössbauer spectra further indicated that the oxidation of the Fe^{2+} ions to Fe^{3+} ions under a magnetic field leaded to the disappear of long-range charge ordering on octahedral sites below T_V because of the absence of Fe^{2+} ions in layers. Fe^{2+} ions could be easily oxidized

to Fe^{3+} ions in order to achieve a higher spin state under a magnetic field in an aqueous solution. The black brown color of Fe^{2+} ions solution experiences a quicker transition to red (Fe^{3+} ions) under 0.25 T compare to the transition without a magnetic field. Under a field intensity of 0.25 T, it is deduced that an enhanced oxidation process could also occur during the chemical synthesis of Fe_3O_4 nanoparticles, leading to the oxidation of Fe^{2+} ions to Fe^{3+} ions on octahedron sites. Therefore, on octahedral sites, the numbers of Fe^{2+} ions and Fe^{3+} ions are different below T_V, resulting in the vanish of charge ordering. This result reveals that the magnetic fields can alter the structure at atomic scales during chemical reaction processes.

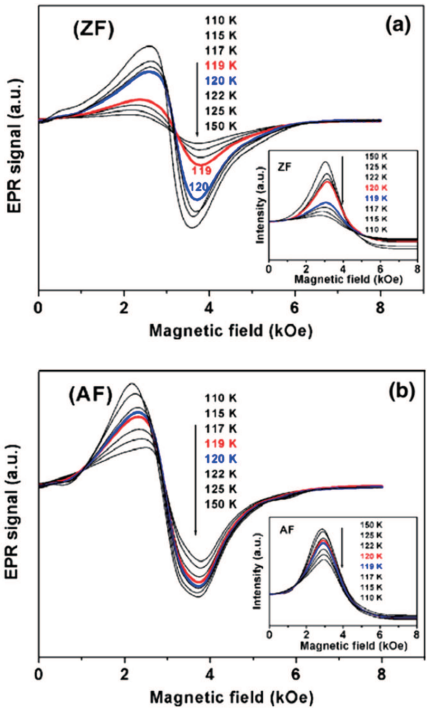


Fig. 10. The EPR results measured at various temperatures for the samples obtained under 0 T (a) and 0.25 T (b). The corresponding integral curves exhibit the same variation tendency, as shown in the insets.[24]

3.7. MFEs on surface spins and activity of catalysts

The MFEs on catalytic reactions have been widely investigated, which shows that the catalytic rate can be controlled by altering the magnetic field intensity. However, the experimental and theoretical work about the MFEs on the activity of nanocatalysts is rarely seen. Pd nanocatalysts have been selected as the model to study the MFEs on the catalytic activity of nanocatalysts. It is suggested that Pd nanocatalysts with the diameter of 2.5 nm are paramagnetic based on their g value of 2.0, and this means that these Pd nanocatalysts may be affected by applied magnetic fields. The catalytic activity of nanocatalysts consisted of Pd nanoparticles and MIL-100(Cr) in the reduction of 4-nitrophenol has been systematically investigated[25] (Fig. 11), which shows that the reduction time is decreased from 2.6 min to 1.4 min under a magnetic field of 0.5 T, indicating the increase of the reaction rate. Moreover, the time of completion for the reaction, t_c, is related with the magnetic field intensities. The t_c gradually decreases from 2.6 min, 2.0 min, 1.8 min, 1.6 min to 1.4 min when the magnetic field intensities increase from about 0 T, 0.2 T, 0.3 T, 0.4 T to 0.5 T. Based on the measurement of ESR spectrum, the Pd nanocatalysts are paramagnetic due to uncanceled surface spins. When a magnetic field is applied, the spin configuration on Pd surface will change from paramagnetic to ferromagnetic. Interestingly, the adsorption of 4-nitrophenol is dependent on the spin arrangement on Pd surface. The magnetic field-induced ferromagnetic configuration will inevitably increase the adsorption number of 4-nitrophenol molecules on the catalyst surface, and then accelerate the reaction rate. The theoretical results further reveal that the change of spin configurations on nanocatalyst surface (paramagnetic convert into ferromagnetic configuration) can reduce adsorption energies in the reaction system. As a result, more 4-nitrophenol molecules could be adsorbed on the nanocatalyst surface (Fig. 12). This shows that the magnetic field can regulate the surface spins configuration which plays significant roles on the catalytic activity. The similar research is worth carrying out under high magnetic fields.

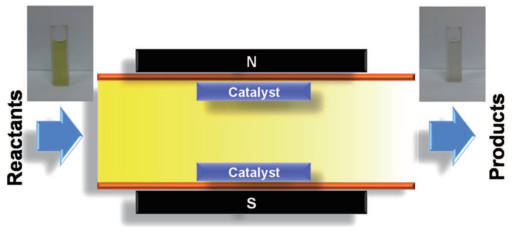


Fig. 11. Schematic illustration of catalytic reaction of 4-nitrophenol under magnetic fields.[25]

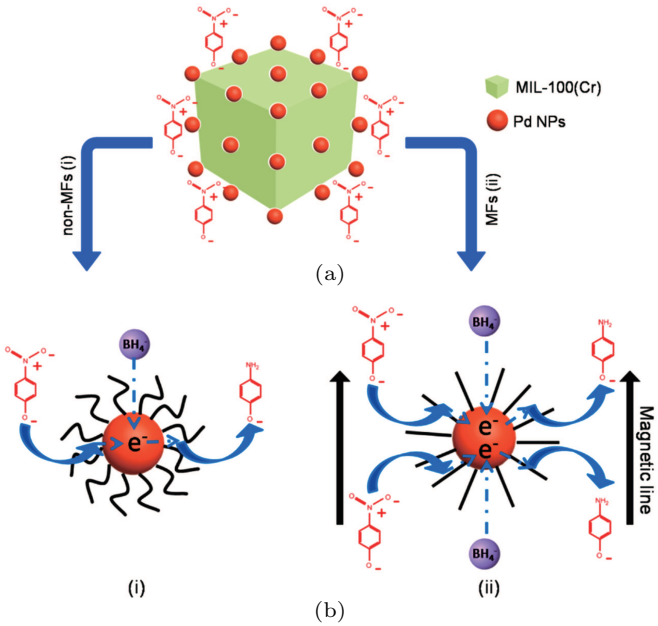


Fig. 12. Schemes of (a) 4-nitrophenol molecules adsorbed on the MIL-100(Cr) surface and (b) 4-nitrophenol reduction on the Pd surface without (i) and with (ii) a magnetic field.[25]

At room temperature, the Suzuki cross-coupling reaction rate is slow even with Pd nanoparticles as catalysts. The MFEs on the Suzuki cross-coupling reaction rate were also investigated in the presence of $Pd@Co_3[Co(CN)_6]_2$ catalysts, which showed that the yield of production can be remarkably influenced at 30 °C (Table 1 and Fig. 13).[26] Moreover, the reaction rate is dependent on the magnetic field intensity. However, the MFEs on the reaction rate become weaker when the temperature increases, and almost disappear at 60 °C. The paramagnetism of Pd nanoparticles is related to the temperature, and the increased temperature will cause the decrease of magnetic susceptibility, which leads to weakening MFEs on the spin at Pd surface. As a result, the advantage produced by MFEs will gradually diminish with the increase of temperature. This result indicates that the magnetic field can act as an external condition to enhance the reaction rates of Suzuki cross-coupling at the lower temperature.

Table 1. At temperature of 30 °C, the yield of the Suzuki reaction in the presence of $Pd@Co_3[Co(CN)_6]_2$ nanocatalyst with and without magnetic fields.[26]

Time/h	2	4	6	8	10	12	24
0 T	13%	19%	25%	29%	32%	35%	44%
0.1 T	15%	23%	31%	35%	38%	40%	49%
0.25 T	16%	31%	37%	40%	42%	45%	54%
0.5 T	17%	32%	40%	45%	50%	54%	65%

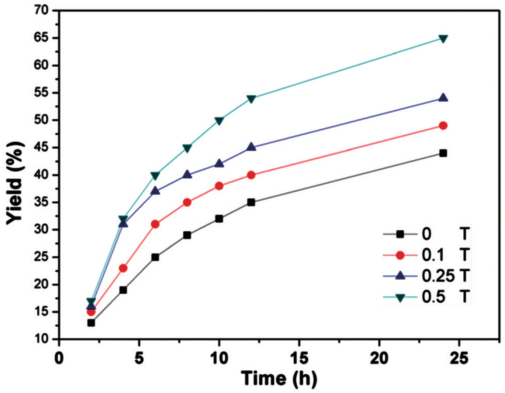


Fig. 13. The curves of the Suzuki reaction yield at 30 °C with and without magnetic fields for different time, respectively.[26]

The density functional theory was employed to gain further insights into the MFEs on the catalytic activity. As we know, in most cases, the adsorption processes are considered as the initial stages for various catalytic reactions. Therefore, the adsorption energies of the reactant molecules on the catalyst surface were calculated by choosing the Pd (111) surface and bri30 conformation as the optimizing model (Fig. 14). Table 2 is the calculated energies of the reactant molecules adsorbed on the above mentioned conformation with and without magnetic fields. The adsorption energy under a magnetic field is lower (−1.12 eV) than that (−1.07 eV) without a field, which results in the change of adsorption behaviors between reactant molecule and catalyst surface. Moreover, due to the decrease of adsorption energy in the reaction process, the stronger chemisorption of bromobenzene molecules on the Pd (111) surface can occur. Therefore, the catalytic activity will be improved because the number of reactant molecules adsorbed on the catalyst surface is increased. Moreover, the analysis of partial density of states (PDOS) was carried out (Fig. 15). Without the magnetic field, one spinous peak has been observed for the 2p orbit in the C atom. In contrast, a more close overlap has been shown under a magnetic field condition, implying the enhanced hybridization between C atoms and Pd atoms. The enhanced hybridization will favor to transfer the electrons from the catalyst substrate to bromobenzene molecules, leading to the increase of the reaction rates of Suzuki cross-coupling. From these studies, one can gain a profound understanding of the MFEs on the surface spin arrangement of nanocatalysts and open a new avenue to control the activities of nanocatalysts by magnetic fields.

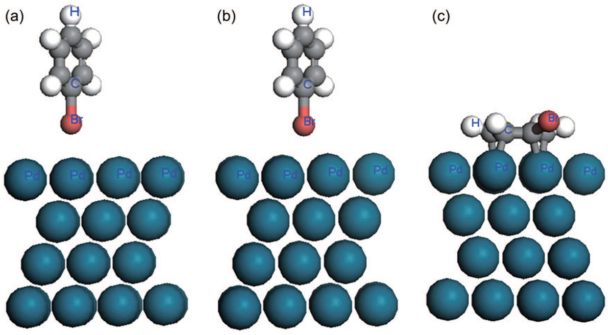


Fig. 14. The different adsorption geometries of bromobenzene molecules absorbed on catalyst surface after geometry optimizations: (a) top site,(b) bridge site, and (c) parallel geometry.

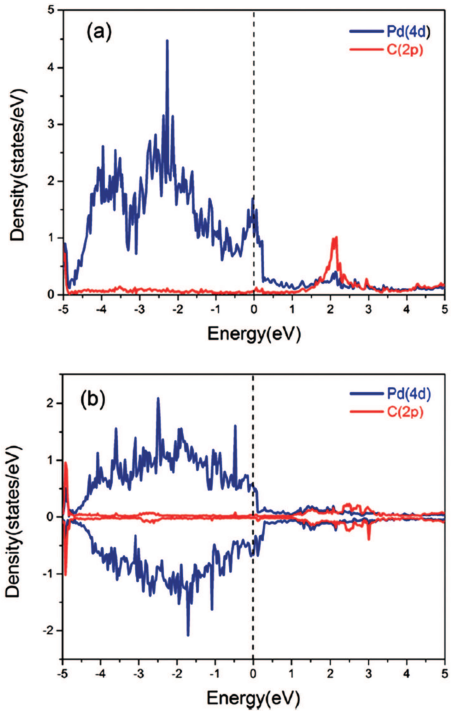


Fig. 15. The partial density states for brombenzene molecules adsorbed on Bri30 site at catalyst surface (a) with and (b) without the magnetic field.[26]

Table 2. Adsorption energies (eV) for brombenzene molecules adsorbed on Bri30 site at catalyst surface with and without magnetic fields.[26]

Energy	Emolecular	Eslab	Eslab+molecular	Eads
No-MFs	–74.11 eV	–176.83 eV	–252.01 eV	–1.07 eV
MFs	–74.11 eV	–176.84 eV	–252.07 eV	–1.12 eV

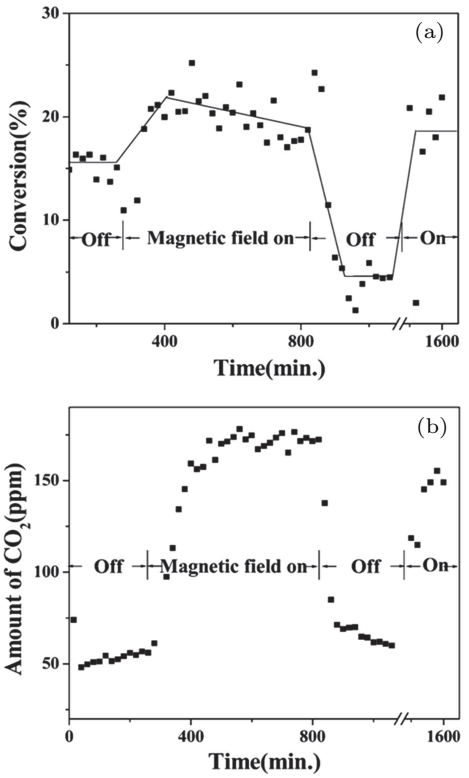


Fig. 16. (a) The MFEs on the photocatalytic conversion of benzene. (b) The MFEs on CO_2 yield for photocatalytic degradation of benzene.[28]

The MFEs research on heterogeneous reaction systems, photocatalysis in particular, is rather interesting and important.[27] For the first time, Fu *et al.* investigated the MFEs on the heterogeneous photocatalytic reaction by degradation of benzene using the Pt/TiO_2 as the catalyst.[28] As shown in Fig. 16, without a magnetic field, the benzene conversion and CO_2 production were 15.5% and 52 ppm at the steady state. Interestingly, when a magnetic field with the intensity of 59.42 mT was employed during the photocatalytic reaction process, the benzene conversion and the CO_2 production could be increased to 18% and 175 ppm, respectively. At room temperature, He *et al.* demonstrated the synergistic effect between nanosized TiO_2 and applied magnetic fields by investigating the degradation of phenol in a photocatalytic reaction.[29] The phenol degradation rate (C/C_0) will be enhanced under magnetic fields with the intensity higher than 0.082 T. In contrast, a low-intensity magnetic field (< 0.044 T) played a negative role on C/C_0. With the raising of magnetic field strength, the yield of hydroxyl radicals increases initially. However, the yield reaches the maximum concentration when the strength is up to 0.082 T. The carriers induced by photo initially decrease when the magnetic field strength is lower than 0.024 T, and then enhance with the increase of magnetic field strength. The MFEs on carriers induced by photo can be interpreted based on the Δg mechanism combined with the hyperfine coupling mechanism. The recombination of holes and electrons can be accelerated and the generation of carriers induced by photo can be suppressed under a magnetic field with low strength, which further limits the phenol degradation. However, the presence of high-strength magnetic field can hinder the hydroxyl radical recombination and thus enhance the hydroxyl radical generation which is the main factor in determining phenol degradation process in the high-strength magnetic field region (Fig. 17).

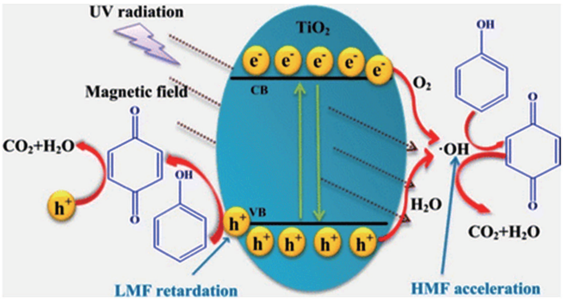


Fig. 17. Effects of applied magnetic fields on the degradation process of phenol over TiO_2 photocatalytic system.[29]

4. Summary and outlook

Over the past decade, in the magnetochemistry, remarkable progress has been made by the researchers in China. However, due to the lack of high magnetic field devices, much work was carried out under weak magnetic fields, which limited the MFEs on reactions involved paramagnetic/diamagnetic substances. According to related formulas mentioned above, the MFEs are dependent on magnetic field intensities. Therefore, the magnetic energy, magnetic force, and other factors in chemical reaction systems will become more remarkable under high magnetic fields. For example, the properties of a multiferroic metal–organic framework with the perovskite ABX_3 architecture could be tuned by a high magnetic field-induced synthesis strategy. Compared to the crystal formed without a magnetic field, the crystal prepared under 9 T exhibits the reduced magnetic susceptibility and ferroelectric polarization value, which is ascribed to the changes of structures (such as hydrogen bond strength, canting angle) induced by the applied high magnetic field.[30] Therefore, there is still a promising opportunity to further pursue magnetochemistry progress with high magnetic fields. Fortunately, in Hefei, the Chinese Academy of Sciences has established a High Magnetic Field Laboratory (HMFL), which will provide an excellent platform for magnetochemistry researches under high magnetic fields. One of water-cooled magnets (20 T) in HMFL possesses a bore diameter of 200 millimeter (Fig. 18).

The large bore diameter is suitable for establishing chemical reaction devices which can be applied to diverse reaction systems under the magnetic field up to 20 T.

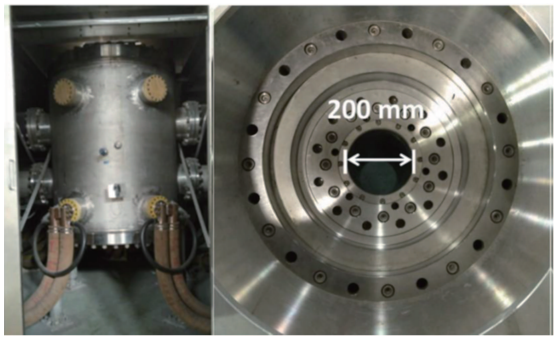


Fig. 18. The water-cooled magnets with bore diameter of 200 millimeter in HMFL.

Several aspects of the work in the future can be suggested as follows. First, high magnetic fields may play significant roles on coordination chemistry reactions, such as the growth of single-molecule magnets (Mn12, Fe8) and multiferroic metal–organic-frameworks (MOFs). Much attention has been paid to multiferroic compounds in which the electric and magnetic properties coexist. In 2009, a family of MOFs with the perovskite structure has been demonstrated to show the multiferroic behavior, which stimulated considerable theoretical and experimental efforts to pursue new hybrid MOFs with multiferroic properties. On the other hand, because of the different origins for magnetic and electric orders, the magnetoelectric coupling effects in multiferroic MOFs are too weak to detect. Therefore, it is high desire to develop a strategy to enhance the magnetoelectric coupling effects in MOFs. It is well known that MOFs possess remarkable structural diversity due to rich coordination modes of organic ligands. As an important extreme condition, the high magnetic fields can transmit high-intensity energy to alter the migration, matching and arrangement of species (such as atoms, molecules, and clusters), leading to the significant impact on size, morphology, structure, and properties of crystals. Therefore, the growth of multiferroic MOFs crystals under high magnetic field may bring remarkable changes. It is expected that new structures of multiferroic MOFs with enhanced magnetoelectric coupling effects will be exploited by controlling coordination modes (reaction pathway, microstructure) with high magnetic fields. Second, the magnetic fields may be employed in chiral selective reactions, such as carbon nanotubes and levo-compounds. For example, as we know, the slight changes of chirality indices in single-walled carbon nanotubes (SWNTs) can lead to the shift of the electrical conductivity from a metallic state to a semiconducting state. However, the chirality purity of SWNTs is hard to gain during the growth process. The carbon radical produced from the decomposition of the carbon feedstock may be affected by applied magnetic fields during a chemical vapor deposition process, and then influence SWNT nucleation and growth, which may lead to the monitoring of reaction pathways that are selective to the chirality. The last, the particular structure with a high catalytic activitiy of noble metals may be constructed via a magnetic field-assisted means. As we know, the selectivity and activity of noble metal catalysts are dependent on the array of surface atoms in most catalytic reactions. The magnetic field with a high intensity could be an alternative condition to regulate surface structures (such as dangling bond and indices of crystal face) of catalysts, and then adjust their catalytic behaviors.

Under high magnetic fields, several scientific subjects of chemical reactions should be investigated: (i) the changes of the conductivity, dielectric constant, the solubility, and pH in reaction media (such as water, organic solvents), (ii) the transport behavior of reactants, (iii) the interactions between high magnetic fields and reactants, (iv) *in-situ* characterization of a chemical synthesis, (v) theoretical simulation of the MFEs on reaction processes.

References

[1] Steiner U E and Ulrich T 1989 *Chem. Rev.* **89** 51
[2] Bull N H 1985 *Chem. Soc. Jpn.* **58** 1088
[3] Wakasa M and Hayashi H 1996 *J. Phys. Chem.* **100** 15640
[4] Brocklehurst B 2002 *Chem. Soc. Rev.* **31** 301
[5] Rodgers C T 2009 *Pure Appl. Chem.* **81** 19
[6] Hu L, Zhang R R and Chen Q W 2014 *Nanoscale* **6** 14064
[7] Wan M X and Yang J 1995 *Synth. Met* **69** 155
[8] Pan H P, Shen Y, Wang H F, He L and Hu B 2015 *Sci. Rep.* **5** 9105
[9] Shao M, Yan L, Pan H P, Ivanov I and Hu B 2011 *Adv. Mater.* **23** 2216
[10] Zhang J Z, Chen Q W and Tao N 2008 *J. Cryst. Growth.* **310** 3788
[11] Hu L and Chen Q W 2012 *Mater. Chem. Phys.* **133** 541
[12] Wang J H, Ma Y W and Watanabe K 2008 *Chem. Mater.* **20** 20
[13] Dong L C, Zhong Y B, Zhe S, Zheng T Y and Wang H 2016 *RSC Adv.* **6** 21037
[14] He Z B, Yu S H, Zhou X Y, Li X G and Qu J F 2006 *Adv. Funct. Mater.* **16** 1105
[15] Cai L, He J F, Liu Q H, Yao T, Chen L, Yan W S, Hu F C, Jiang Y, Zhao Y D, Hu T D, Sun Z H and Wei S Q 2015 *J. Am. Chem. Soc.* **137** 2622
[16] Tongay S, Varnoosfaderani S S, Appleton B R, Wu J and Hebard A F 2012 *Appl. Phys. Lett.* **101** 123105
[17] Geng X M, Sun W W, Wu W, Chen B, Al-Hilo A, Benamara M, Zhu H L, Watanabe F, Cui J B and Chen T 2016 *Nat. Commun.* **7** 10672
[18] Wang J, Chen Q W, Zeng C and Hou B Y 2004 *Adv. Mater.* **16** 137
[19] Pol V G, Pol S V, Calderon-Moreno J M, Sung M G, Asai S and Gedanken A 2006 *Carbon* **44** 1913
[20] Xu Y B, Ren Z M, Ren W L, Cao G G, Deng K and Zhong Y B 2008 *Nanotechnology* **19** 115602
[21] Wang M S and Chen Q W 2010 *Chem.-Eur. J.* **16** 12088
[22] Sun L X and Chen Q W 2009 *J. Phys. Chem. C* **113** 2710
[23] Sun L X, Chen Q W, Tang Y and Xiong Y 2007 *Chem. Commun.* **27** 2844
[24] Wang J, Chen Q W, Li X G, Shi L, Peng Z M and Zeng C 2004 *Chem. Phys. Lett.* **390** 55
[25] Li R, Yang Y, Li R and Chen Q W 2015 *ACS Appl. Mater. Interfaces.* **7** 6019
[26] Gao L, Wang C L, Li R, Li R and Chen Q W 2016 *Nanoscale* **8** 8355
[27] Okumura H, Endo S, Joonwichien S, Yamasue E and Ishihara K N 2015 *Catal. Today* **258** 634
[28] Zhang W, Wang X X, Fu X Z 2003 *Chem. Commun.* **17** 2196
[29] He C, Liu X H, Ji W J and Zhao J L 2016 *Water Air & Soil Pollution* **227** 99
[30] Hu L, Wang Z, Wang H, Qu Z and Chen Q W 2018 *RSC Adv.* **8** 13675